The Carbonate Platform Model and Reservoirs' Origins of the Callovian-Oxfordian Stage in the Amu Darya Basin, Turkmenistan

Wenli Xu [1,*] [ID], **Huaguo Wen** [1,*], **Rongcai Zheng** [1], **Fengjie Li** [1], **Fei Huo** [2], **Mingcai Hou** [1] **and Gang Zhou** [3]

1   Institute of Sedimentary Geology, Chengdu University of Technology, Chengdu 610059, China; zhengrc@cdut.edu.cn (R.Z.); lifengjie72@163.com (F.L.); houmc@cdut.edu.cn (M.H.)
2   School of Geosciences and Technology, Southwest Petroleum University, Chengdu 610500, China; huofei342099206@163.com
3   Exploration and Development Research Institute of PetroChina Southwest Oil & Gasfield Company, Chengdu 610051, China; zhougang29@126.com
*   Correspondence: xuwenli5@163.com (W.X.); wenhuaguo08@cdut.cn (H.W.); Tel.: +86-159-2800-2838 (W.X.); +86-028-8407-9807 (H.W.); Fax: +86-028-8407-9807 (H.W.)

Abstract: The Calloviane-Oxfordian carbonates in the northeastern Amu Darya Basin of southeastern Turkmenistan are composed of medium- to thick-bedded, mostly grainy limestones with various skeletal (bivalves, brachiopods, echinoderms, foraminifera, corals, and sponge) and non-skeletal grains (intraclasts, ooids and peloids). Two facies zones, six standard facies belts and some microfacies types were recognized, and sedimentary model "carbonate ramp-rimmed platform" was proposed and established that can be compared with the classical carbonate sedimentary models. In this model, favorable reservoirs not only developed in the intraplatform shoal of open platform, or reef and shoal on the platform margin, but also in the patch reefs, shoal and mound facies on the upper slope. The reservoir's pore space is dominated by intergranular and intragranular pores and fissure-pore reservoirs exist with medium porosity and medium to low permeability. Sedimentary facies and diagenetic dissolution are the key controlling factors for the development of high-quality reservoirs.

Keywords: sedimentary model; Callovian-Oxfordian; Amu Darya Basin; reservoir; main controlling factors

1. Introduction

With the constant increase of China's demand on energy resources and theory advancement in oil and gas exploration, some major discoveries of oil and gas exploration have been made in marine carbonates of the Tarim, Sichuan and Ordos basins. Subsequently, marine carbonate has become an important domain of exploration in China, and petroleum geological characteristics of carbonate platform have become a new hotspot of research [1]. High-efficiency oil and gas exploration in marine carbonates requires the guidance of the sedimentary model. Studies on carbonate sedimentary evolution and models commenced in the 1960s. Shaw (1964) [2] first introduced the concepts of epicontinental sea and marginal sea and laid the foundation for the carbonate sedimentary model. Since then, many scholars have come up with new ideas on controlling factors and depositional models of carbonate sedimentation from the aspects of sea level variation, marine environment, climatic conditions and structural settings [3–18], which enriched and developed the research contents of the carbonate sedimentary model. As oil and gas exploration progressed, in practice, it is still difficult to characterize the carbonate platform in detail with a certain model, although achievements have been

made in analogy study with the application of existing models. Therefore, the only method applicable is to build a carbonate sedimentary model suitable for the study area through analysis, correlation and summarization of real data, to guide oil and gas exploration practices. Based on existing carbonate sedimentary models proposed by researchers before [19–21] and the author's understandings of the Callovian-Oxfordian marine carbonates in the Amu Darya Basin, Turkmenistan, a new carbonate sedimentary model applicable to this basin has been proposed. The development conditions and distribution law of reservoirs in this basin have been analyzed by using this model, in the hope of providing the basis for oil and gas exploration of the Middle-Upper Permian and Middle-Lower Triassic strata in the Middle-Upper Yangtze region that share similar carbonate sedimentary model and reservoir origin in the Callovian-Oxfordian strata in the Amu Darya Basin.

2. Geological Setting

Located in the northeastern part of Turkmenistan, southern part of Uzbekistan and northwestern part of Afghanistan, the Amu Darya Basin is one of the most important hydrocarbon basins in the Central Asia region [22], as well as the source of China's West-East gas transmission project. Structurally, it is a large-scale Mesozoic superimposed basin situated in the southeastern part of the Turan Platform on the Sino-Korea-Tarim Plates, within the Tethys structural domain in the central-western parts of the Central Asian structural belt (Figure 1) [23–26]. The Amu Darya Basin has experienced three stages of evolution: the rifting stage during the Permian to Triassic periods, the steady subsidence stage from the Jurassic to Cretaceous periods, and the uplifting and reforming stage during the Paleogene-Quaternary periods. From the Late Permian to Triassic periods, the subduction of Tethys Ocean into the Eurasian plate enabled the formation of the back-arc extensional rift and, under the extensional tectonic setting, fault terrace belt was formed in the basin, thereby laying the foundation for steady subsidence of the basin. From the Jurassic to Cretaceous periods, a critical period for the formation of the basin, the basin subsided steadily, with relatively weak tectonic movements and absence of faults, and the thickness of the strata deposited increased from west to east, but the variation is small. Tectonic movements occurred during this period have a strong control on the formation and development of source rocks, reservoirs and caprocks in the basin (Figure 2a–c). From the Paleogene to Quaternary periods, in response to the Alpine movement and the neotectonics, folds in the eastern and northeastern parts of the basin were uplifted, the basin was divided into the north and south two depression zones by a salt dome structural belt in the middle. In addition, tectonic framework of the fault terrace belt surrounding the basin and the placanticline uplift belt within the basin was eventually formed (Figure 2d) [27,28]. On the whole, the Amu Darya Basin is surrounded by fold mountain systems and deep-large faults. It is bordered to the northeast by the Kyzylkum High Belt, to the southeast by the southwest branch range of the Gissar mountains and the Bande Turkestan Foldbelt, and to the southwest by the Kopet-Dag Foldbelt. With a series of uplifts, depressions and paleo-anticlines in the middle, and the margin plunging towards the hinterland in a ladder-like mode, the basin generally takes on a NW-SE trending dustpan shape that is narrow and steep in the south and west wings and wide and gentle in the north and east wings (Figure 1). The basin is divided into three first-order structural units, according to structural morphology of the basement and the sedimentary strata: the Kopet-Dag piedmont depression belt in the southwestern part, the Karakum High in the central part and the Amu Darya Depression belt in the northeastern part [29,30]. Regional tectonic-sedimentary framework and distribution of reservoirs, caprocks and gas pools are controlled by the NW- and NE-trending faults developed in the basin [31].
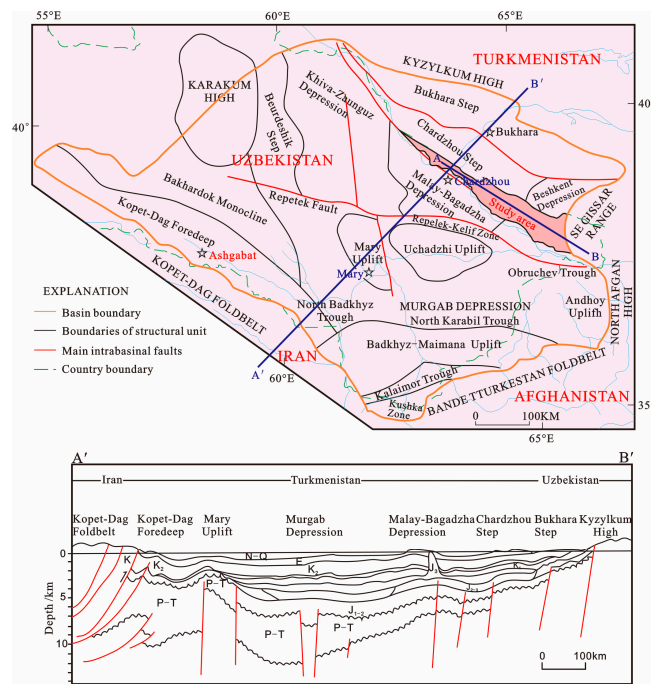
Figure 1. Overview of regional structure in the Amu Darya right bank area.
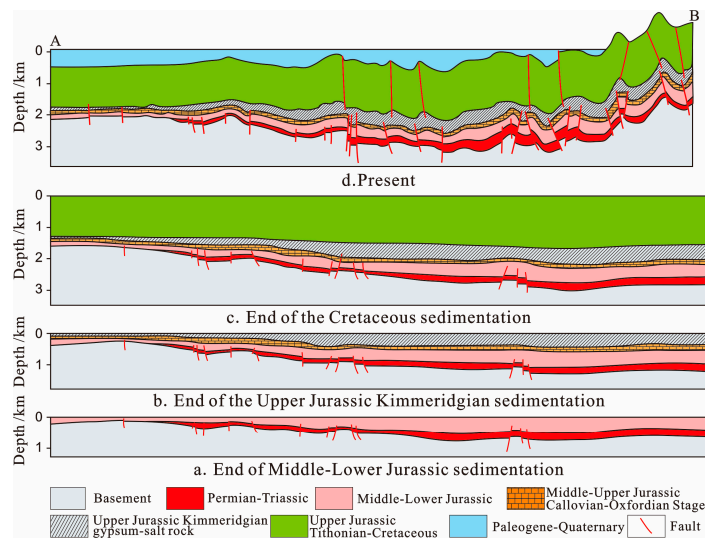

Figure 2. Palinspastic sections in Amu Darya Basin, location of profile is shown in Figure 1 (Reference [27,28]).

The study area is located in the right bank of the Amu Darya, Turkmenistan (Figure 3), and structurally is part of the Chardzhou terrace in the Amu Darya Basin. The Amu Darya basin contains three structural bed series with different structural and sedimentary characteristics: i.e., the basement, transition bed and sedimentary bed. The basement is composed of the Paleozoic volcanic and metamorphic rocks and its burial depth varies greatly. The transition bed consists of the Permian-Triassic terrigenous clastic rocks, with thickness increasing from north to south. The sedimentary bed is comprised of the Jurassic, Cretaceous and Paleogene carbonates, evaporites and interbedded sandstone, mudstone and coal bed [32–34]. The Middle-Upper Jurassic Callovian-Oxfordian stratum, consisting of a carbonate sedimentary assemblage [34–37], is the most important hydrocarbon-bearing formation in the basin. It is in unconformable contact with the

underlying the Middle-Lower Jurassic coal-bearing clastic rock that can act as source rock, and in conformable contact with the overlying Upper Jurassic Kimmeridgian gypsum-salt rock that can act as tight caprock. The Callovian-Oxfordian stratum can be divided into eight layers according to lithologies XVI, XVa2, Z, XVa1, XVhp, XVm, XVp, XVac and three sedimentary sequences with a complete regional transgressive-regressive cycle (SQ1, SQ2, SQ3) (Figure 4). Of these sequences, SQ1 is composed of four lithologic layers (XVI, XVa2, Z, XVa1) that are equivalent to the Callovian, SQ2 consists of three lithologic layers (XVhp, XVm) that are equivalent to the early-stage of the Oxfordian, and SQ3 is comprised of two lithologic layers (XVp, XVac) that are equivalent to the later-stage of the Oxfordian. Basically, lithological layers of these three integral sequences correspond well with the sedimentary system tracts that span various sedimentary facies belts and hence can be correlated on a regional scale, although these sequences differ in regional lithology, lithofacies and thickness (Figure 5).
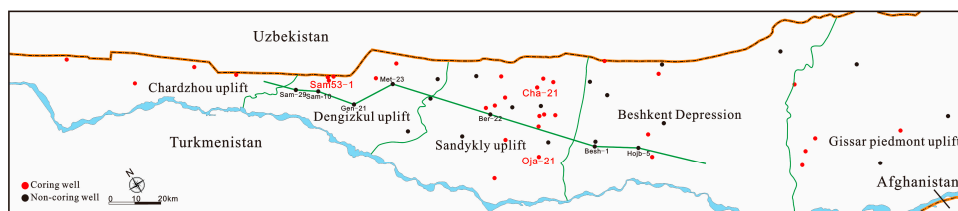

Figure 3. Distribution of wells in Amu Darya right bank area.
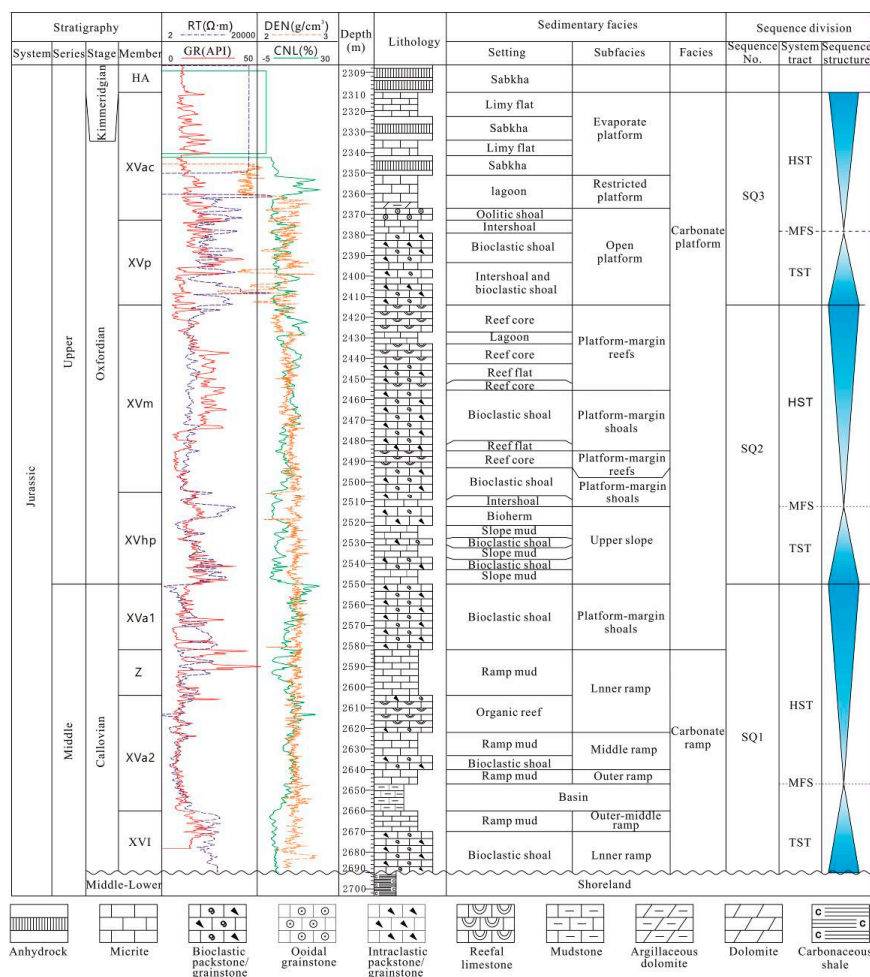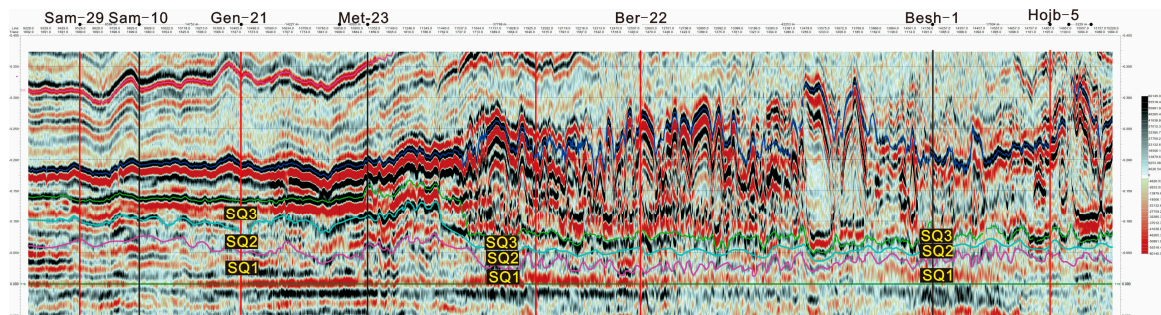

Figure 4. Lithological, chronostratigraphy and stratigraphic sequence of Callovian-Oxfordian Stage in Amu Darya Basin.

Figure 5. Sequence stratigraphy and seismic characteristics of Callovian-Oxfordian Stage, location of profile is shown in Figure 3 (Reference [38]).

3. Samples and Method

Detailed petrographic studies were based on approximately 800 thin sections (Figure 1) stained with Alizarin Red S and potassium ferricyanide solution [39]. Carbonate rocks were classified by following the nomenclature of carbonate rocks by Dunham (1962) [40]. Depositional sequences and inferred relative sea level changes were interpreted based on the Carrozi method [41]. Facies identification and stacking patterns of facies followed the classification of Tucker and Wright (1990) [42], Flügel (2010) [43]. Sedimentary system tracts were defined based on facies trends, stacking pattern, lithological changes, and nomenclature by following Vail (1977a, 1977b) [44,45] and Wang (2014) [38]. These sequence-stratigraphic tracts were then correlated with each other based on facies and depositional environments and finally related to the global sea level curves of Haq (1988) [46]. In this paper, division of sedimentary facies was based primarily on the carbonate sedimentary model proposed by Wilson (1975) [5], Tucke (1981) [7], Basilone (2016) [16], and secondly on the model proposed by Mcllreath and James (1979) [6], and Read (1985) [9]. Core samples used in this study were recovered from the Callovian-Oxfordian in the right bank of the Amu Darya, Turkmenistan. These carbonate samples were utilized for thin section, porosity-permeability and mercury injection analyses.

Physical properties and mercury injection tests were conducted on cylinder shape samples (25 mm long and 25 mm in diameter), with CMS-300 tester (Core Lab, Houston, State of Texas, USA) for testing porosity and permeability under overburden pressure and AutoPore IV 9500 mercury injection apparatus (MICROMERITICS INSTRUMENT CORP, Atlanta, GA, USA), in accordance with SY/T6385-1999 and SY/T 5346-1994, and undertaken by Key National Lab of Oil and Gas Reservoir Geology and Development Engineering, Chengdu University of Technology. The detail data were presented in Supplementary Table S1.

X-ray diffraction analysis was conducted by using D/MAX-IIIC diffractometer (Rigaku Corporation, Tokyo, Japan), in accordance with JCPDS-ICDD, and was undertaken by Key National Lab of Oil and Gas Reservoir Geology and Development Engineering, Chengdu University of Technology. The detail data were presented in Supplementary Table S2.

Electron probe X-ray microanalysis was conducted by using EPMA-1720 H Series Probe microregion analyzer (SHIMADZU, Kyoto, Japan) and INCA Energy 250 X-Max20 energy disperse spectroscopy (SHIMADZU, Kyoto, Japan), and was undertaken by Key National Lab of Oil and Gas Reservoir Geology and Development Engineering, Chengdu University of Technology.

## 4. Sedimentary Characteristics and Models of Carbonates

4.1. Sedimentary Characteristics

By observing and characterizing cores recovered from 33 wells and conducting well log interpretation of several non-coring wells, in combination with preexisting research data of sedimentary sequence, lithofacies paleo-geography and petroleum geological characteristics [33–38,47–54], it is

found that, under the control of the paleo-geomorphology high in northwest and low in southeast, a set of carbonate rock with distinct features of deep- and shallow-marine facies was deposited in the study area. The distribution framework of facies belt and basic characteristics of each facies belt are as follows.

Shallowwater platform facies zone in the northwest of the study area contains platform evaporitic, restricted platform, open platform and platform margin. Platform evaporitic is present in the XVac layer only, the lithology is dominated by massive anhydrock with crystal grain structure (Figure 6a), intercalated with anhydrite-carbonate dolostone and mudstone. Restricted platform is present primarily in the XVac and XVp layers, and is dominated by interbedded grey to dark grey thin-bedded micrite (Figure 6b) and microbioclastic, intraclastic wackestone. Open platform is present broadly in various layers, consisting of platform interior restricted and shoal with alternating sequences, and is dominated by grainstone deposited in high-energy shoal environment, such as well-sorted micrite, ooidal grainstone (Figure 6c) and bioclastic grainstone, and alternatively developed micrite and bioclastic wackestone deposited in low-energy environment. In this facies belt, a large variety of biotypes were present, including the actinozoan, echinodermata, bryozoan, foraminifer, gastropods, bivalve and algae. Platform margin zone depositing in strong hydrodynamic force include two types, marginal reef and shoal, and is dominated by the assemblage of well-sorted grainstone (Figure 6d), bioclastic and ooidal–grainstone with isopachous rimmed cementing structure, and rudist bivalve framestone and boundstone (Figure 6e), with the rudist bivalve being the primary reef-building organism, as well as a small amount of sponge boundstone (Figure 6f), Ceriocava boundstone (Figure 6g), stromatoporoids boundstone, coral boundstone and coral-rudist bivalve framestone, intercalated with a little bioclastic packstone/wackestone. Some typical accessory reef organisms present commonly in this facies belt include benthic foraminifera, brachiopoda, gastropods, algae, Echinodermata and bivalve. In seismic profile, marginal shoal body is represented by the wavily changed events, with amplitude, frequency and phase changed accordingly; reef body is represented by the mound-like inclined reflection of moderate to high amplitude, with high amplitude on top, and low frequency, weak amplitude, and disordered and lenticular reflection inside, and is relatively steep towards the sea and flat-gentle towards the land; and the shoal facies is generally represented by worm-like and wavy-like reflections (Figure 7).

Deepwater front slope and basin facies zones are situated in the southeast of the study area. In the slope facies zone, intraclastic packstone (Figure 6h), bioclastic packstone, organic boundstone and micrite occur in the upper slope, while micrite, intercalated with a small amount of microbioclastic wackestone and mudstone, deposited on the lower slope. Bioclasts are dominated by sponge spicule and radiolarian. On seismic section, slope facies is commonly represented by the parallel continuous reflection with low frequency, and is thinner than the platform and platform margin facies. Interestingly, mound-like or amygdaloidal or irregular reef-shoal anomalies are commonly seen under the strong amplitude and disorder reflection background on the upper slope (Figure 7), leading to considerable increase of formation thickness. The basin facies zone is dominated by micrite and mudstone, intercalated with dark shale.
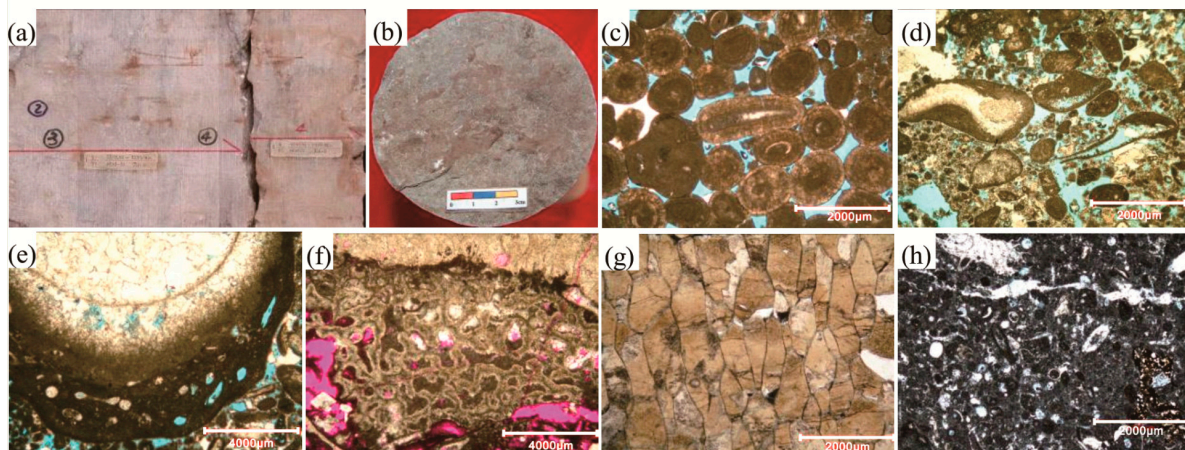
Figure 6. Paleontologic characteristics and various carbonate rock types of Callovian-Oxfordian Stage. (**a**) Grey white gypsum rock, 2247.45–2247.92 m, XVac, Well NFar-21, platform interior evaporitic; (**b**) Micrite, 2377.06–2377.29 m, XVp, Well Sam53-1, restricted platform; (**c**) Ooidal grainstone, 2372.69 m, XVac, Well Sam53-1, open platform interior oolitic shoal, casting thin section (-); (**d**) Bioclastic grainstone, with bioclasts dominated by rudist bivalve, foraminifer, metacrinus, brachiopoda, bryozoan and red alga, 2447.92 m, XVm, Well Sam45-1, platform marginal shoal, casting thin section (-); (**e**) Rudist bivalve framestone, 2454.76 m, XVm, Well Sam53-1, platform marginal reef, casting thin section (-); (**f**) Sponge boundstone, 2459.42 m, XVm, Well Sam53-1, platform marginal reef, casting thin section (-); (**g**) Bryozoan boundstone, bryozoan is istulipora, 2439.85 m, XVm, Well Sam53-1, platform marginal reef, casting thin section (-); (**h**) Intraclastic packstone, with a little ostracoda, foraminifer, bryozoan and echinodermata, XVhp, 3557.4 m, Well Shi-21, upper slope, casting thin section (-).
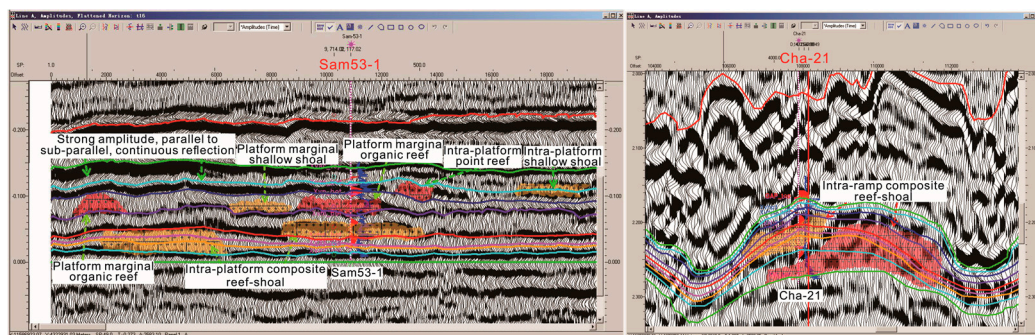
Figure 7. Interpretation of facies types based on seismic profiles in Samendepe and Chashgui areas, well sites are in Figure 3 (Reference [37]).

4.2. Sedimentary-Sequence Evolution Characteristics of Callovian-Oxfordian

It is indicated from the feature of basin margin that the basement of the Amu-Darya Basin is a Hercynian accreted terrane composed of two large Precambrian continental massifs (micro- continents in pre-collisional structure) expanding northwardly and southwardly and Paleozoic metamorphosed rocks [29,55]. In Late Permian-Triassic (possibly Late Triassic/Early Jurassic [56]) the Iranian Block collided with the southern margin of Eurasia, and the Paleotethys Ocean was closed [29,57,58]. A series of structural faults formed in the collision event separate the basement of the basin into numerous paleo-uplifts and graben structures [59–62]. Hereafter, the Amu-Darya Basin entered the development stage of rift basin [63] and a period of stable settlement. In Lower-Middle Jurassic, there were the clastic sediments with greater thickness [64], which were unconformably contacted with the underlying stratum [65]. In Middle Jurassic Bathonian Stage/Callovian Stage, there was large-scale transgression,

and the successive paleo-uplifts (e.g., Chardzhou, Dengizkul, Sandykly) and basement faults in the basin controlled the deposition of carbonates in this period [14–18]. During the deposition of Callovian stage, affected by the basement and Permian to Triassic tectonic movements, paleo-geomorphology of the study area remained high in the northwest and low in the southeast, and the water depth increased gradually from the northwest to southeast, the paleo-uplifts were situated within the relatively deepwater zone, while a broad area to the west of the Chardzhou uplift was the shallowwater zone, slope-break belt was absent, the paleo-geomorphology was relatively gentle and flat, and carbonate sedimentation exhibited the ramp model. During the Oxfordian sedimentation, the overall water depth was shallower than that during the Callovian sedimentation, paleo-uplifts exhibited differential sedimentary characteristics due to the influence of water depth; the water depth increased successively from northwest to southeast, that is, Chardzhou paleo-uplift → Dengizkul paleo-uplift → Sandykly paleo-uplift → Beshkent depression (Figure 3). The Dengizkul paleo-uplift was located in the transition zone from the shallowwater to deepwater, was the conjunction between the transfer zone in the central Sandykly and the weak tectonic deformation belt in the western Sandykly, and was uplifted higher than other paleo-uplifts. At that period, the Dengizkul paleo-uplift had high hydrodynamic energy and abundant nutriments, enabling large-scale growth of organic reef, and carbonate sediments were characterized by the rimmed platform model. Sedimentary-sequence evolution characteristics of the Callovian-Oxfordian are as follows.

4.2.1. Sedimentary-Sequence Evolution Characteristics of Callovian

The Callovian is an integral sedimentary sequence 80 to 330 m thick made up of a transgressive system tract and a highstand system tract, exhibiting an asymmetric structure of rapid transgressive and slow regression (SQ1 in Figure 4). The transgressive system tract is mainly in the XVI layer. Affected by the paleo-geomorphology of the study area high in the northwest and low in the southeast and a rapid transgression over a broad range, marine carbonate rocks retrograded from southeast to northwest and onlapped the Middle-Lower Jurassic clastic continental shelf, the difference between the primary form of the carbonate ramp and the sedimentary framework of the inner ramp, mid-ramp, outer ramp and basin facies began to emerge. The lithology is dominated by interbedded dark grey thin-medium micrite and bioclastic wackestone. Aggradation during the maximum flooding period (or condensed member) is present in the lower part of XVa2, and the lithology is grey black thin-bedded marlstone intercalated with dark shale of mid-outer ramp and basin facies. Early-stage sediments of highstand system tract are in the middle and upper parts of XVa2 and Z, which retain the differential sedimentary frameworks of inner ramp, mid-ramp, outer ramp and basin facies, but relatively large-scale progradational shallow shoal and organic reef began to form at the front of the inner ramp (Figures 4 and 8a), and the lithology is dominated by non-isopachous assemblage of bioclastic wackestone, bioclastic packstone and reefal packstone. Later-stage sediments of highstand system tract deposited in XVa1, as the sea level fell, carbonate ramp break began to transform into the carbonate platform, forming a sedimentary framework with obvious differentiation from the shallowwater facies zone to deepwater facies zone, that is, from the margin to the center of the basin, open platform → platform margin → front ramp → basin facies (Figures 4 and 8b). It is noteworthy that the platform marginal organic reef and shoal facies belts with intensive progradation effect were developed within the border of Uzbekistan north in the study area, and the main part of the study area was situated in the platform marginal ramp → deepwater facies belts of the basin at this period. The event of great significance is the commencement of the formation of shoal and organic reef with intensive progradation effect in the upper part of the shallowwater ramp in relatively shallowwater, and the lithology is dominated by the assemblage of grey medium to thick-bedded sparry bioclastic grainstone and massive reefal packstone intercalated with medium to thin-bedded bioclastic wackestone.
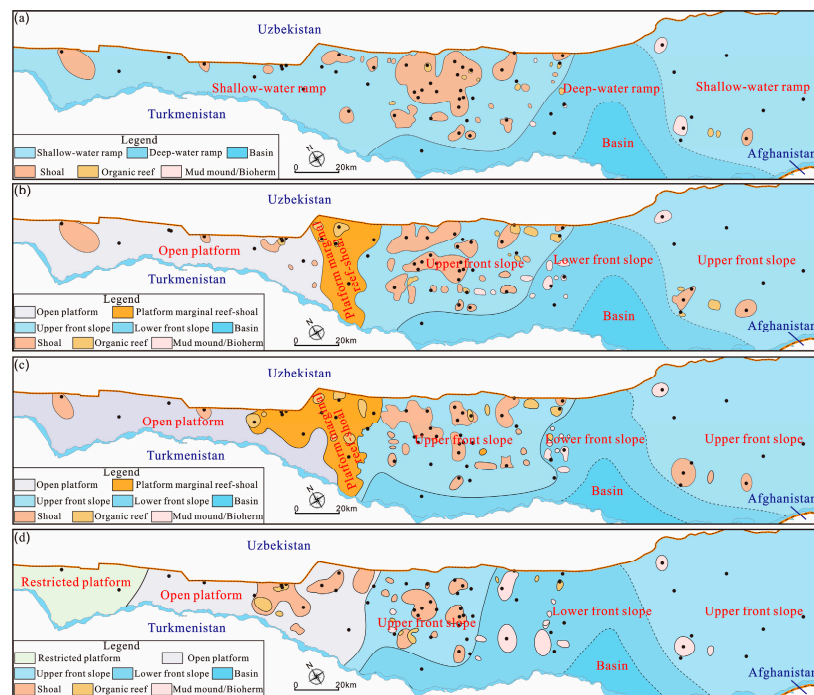
Figure 8. Sketch map showing distribution of sedimentary facies and paleogeography of Callovian-Oxfordian Stage in Amu Darya Basin ((**a**) layer XVa2; (**b**) layer XVa1; (**c**) layer XVm; (**d**) layer XVp)).

### 4.2.2. Sedimentary-Sequence Evolution Characteristics of Oxfordian

Two integral sedimentary sequences were formed in the Oxfordian, each of which consists of transgression and highstand system tract and possesses the asymmetric structure of rapid transgression-slow retrogression (SQ2 and SQ3 in Figure 4). The first sedimentary sequence (SQ2) includes the XVhp-XVm layers, with the thickness of 10 to 180 m. Under the control of the global "Oxfordian transgression", sea level rose rapidly during the early stage of Oxfordian, transgressive system tract was formed in the XVhp layer, which kept the rimmed platform sedimentary framework of SQ1 highstand system tract at late stage, i.e., open platform → platform margin → front ramp → basin facies, and the lithology is dominated by the non-isopachous interlayer assemblage of grey, medium to thick-bedded bioclastic grainstone, massive reefal packstone and medium to thin-bedded bioclastic wackestone. Sediments deposited during the maximum transgression period (or condensed member) are present in the upper part of the XVhp layer, and the lithology is dominated by grey thin-bedded micrite of front ramp facies. Highstand system tract was formed in the XVm layer, the sedimentary framework retained the previous open platform → platform margin → front ramp → basin facies (Figure 8c). In addition, as sea level fell slowly and reefs and shoals commonly grew and accumulated rapidly, the growth of reefs and shoals reached the largest scale in the whole Callovian-Oxfordian. As a result, reefs and shoals were widespread at the platform margin, and large-scale aggradational shallow shoals and point reefs were commonly present on the upper front ramp, and the lithology is dominated by non-isopachous interlayer assemblage of micrite, bioclastic wackestone/packstone, intraclastic packstone and reefal packstone.

The third sedimentary sequence (SQ3) consists of the XVp-XVac layers, with a thickness of 10–140m. The transgressive system tract was formed mainly in the XVp layer. The sea level remained low in the study area due to the shallow depth and relatively closed water body, although transgression occurred rapidly; sediments of platform marginal reef and shoal facies didn't develop any more, and the sedimentary framework was restricted platform → open platform → front slope → basin facies, from the margin to the center of the basin (Figure 8d). Large-scale shallow shoal with intensive aggradation → progradation still developed in the upper part of platform front slope, and the lithology

is dominated by the assemblage of grey medium to thick-bedded bioclastic grainstone and intraclastic grainstone intercalated with medium to thin-bedded bioclastic wackestone. Aggradation of the maximum flooding period (or condensed member) occurred in the upper part of the XVp layer, and the lithology is grey thin-bedded micrite of open platform facies. Highstand system tract sediments were developed in the XVac layer. As sea level fell considerably, the sedimentary framework of platform interior evaporitic → restricted platform → open platform → front slope → basin facies was formed gradually from the margin to the center of basin. It is noteworthy that, the so-called basin facies sediments in this framework refer to the deep lagoon with closed bay, of which the lithology is dominated by thin-bedded high-gamma mudstone intercalated with a few thin-bedded grey black marlite. Its origin is related to the direct transition of deepwater basin into deep lagoon driven by the intensive limitation to seawater circulation resulted from the rapid and considerable sea level fall occurred at the end of the Oxfordian.

4.2.3. Sedimentary Model

Since the epicontinental sea fresh-water carbonate sedimentary model was first proposed by Shaw (1964) in the 1960s, the research related to the carbonate sedimentary model has been enriched and developed constantly [1–18] over the past 50 years, but the current available models are inapplicable to lithofacies paleo-geography research of the Callovian-Oxfordian in the Amu Darya Basin. Similar situation happened in the Upper Paleozoic and Mesozoic marine carbonates in the Sichuan Basin too. Therefore, based on the carbonate sedimentary models proposed by Wilson (1975) [5], Mcllreath and James (1979) [6], Tucker (1985) [8], Read (1985) [9], Gu (2007) [1], Basilone (2016) [16], in combination with the sedimentary characteristics of the Callovian-Oxfordian in the Amu Darya Basin, the sedimentary model of "carbonate ramp-rimmed platform" has been proposed (Figure 9).
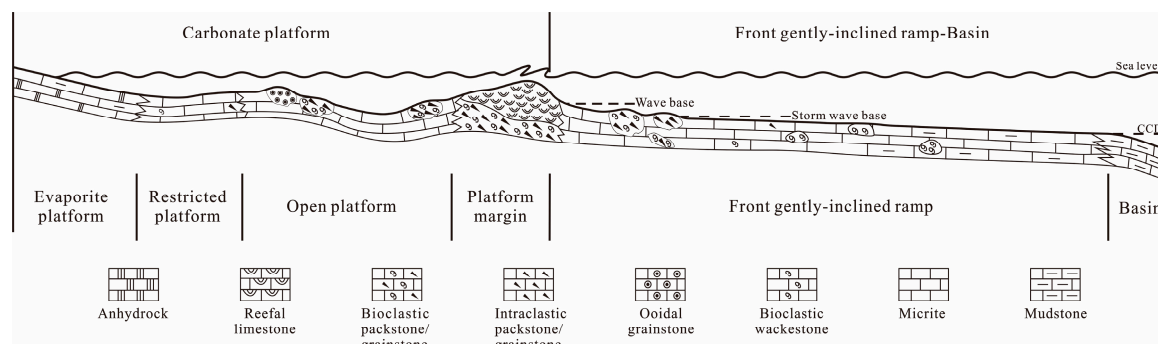
Figure 9. A sedimentary model of carbonate ramp (gently inclined slope) and rimmed platform of Callovian-Oxfordian Stage in Amu Darya Basin (Reference [8,16]).

1　Concept of sedimentary model of "carbonate ramp-rimmed platform"

In this study, this sedimentary model of "carbonate ramp-rimmed platform" is defined as open shallow shelf marine domain, where the sedimentation is dominated by carbonate, carbonate shelf is rimmed with reef and shoal facies, and wide and gentle slope is present in the transition zone between shelf and deepwater basin. In general, the domain can be subdivided into two sedimentary facies provinces, including six facies belts and several microfacies (Figure 9). According to the model proposed by "Tucker (1985) [8]", these two sedimentary facies provinces are named the carbonate shallowwater platform sedimentary province and the front ramp-basin deepwater province, and the six standard facies belts include the platform evaporitic, restricted platform, platform margin, front ramp and basin.

2　Characteristics and evidence of the sedimentary model of "carbonate ramp-rimmed platform"

Original version of this model was first proposed by Gu (2009) [1] based on development characteristics of Great Barrier Reef in Australia, which is named the "open ramp-rimmed platform". The sedimentary model of "carbonate ramp-rimmed platform" proposed by the authors [29] on the basis of the development characteristics of the Callovian-Oxfordian carbonates has two evident sedimentary characteristics and evidences.

(1)   Width and dip of slope

Of over 140 wells penetrating the Callovian-Oxfordian in the study area, around 90 encountered the front slope facies belt in the XVa1-XVm layers. Based on core data and well log data of the coring interval, as well as seismic data, the carbonate rimmed platform commenced broad development during the XVa1-XVm sedimentation, and the width of the front slope commonly exceeded 350 km, much greater than the average width (70 km) of the modern marine slope. Within a distance of 60 km from the Tan wellblock to Besh wellblock on the upper front slope, thickness of the XVa1-XVm increases from 60 to 90 m, indicating a relatively small variation in slope inclination, which is consistent with the tectonic evolution characteristics of Callovian-Oxfordian obtained by Zhang [27] through the analysis based on the principle of balanced section (Figure 2b). Therefore, it is speculated that the front slope belt in the study is different from normal platform in two aspects: (1). the front slope belt is quite wide and gentle; (2). although slope break belt with gradually deepening water body is present between platform margins, the sedimentary characteristics of slope break belt, particularly the landform-controlled gravity flow sediments, are absent.

(2)   Development scale of reefs and shoals

In the study area, other than platform margin facies belt, large-scale and continuously distributed shoals were developed in the upper part of front slope belt, with point reefs and bioherm groups locally, and the lithology is dominated by bioclastic packstone/grainstone and intraclastic packstone/grainstone, intercalated organic boundstone and reefal packstone. Similar features are described from the seaward front of marine sand belt adjacent to the reef environment of NW Sicily, Florida and Bahamas modern carbonate platform [16,66–68]. The Sicily Island and other platform margin reef front-upper slope mainly contain the deposition of oolitic limestone and bioclastic limestone, and shoal bodies show obvious lateral distribution and slightly narrower longitudinally [16]. It can be seen from lithologic characteristics and development scale of reefs and shoals that the formation of reef-shoal assemblage in front slope over 350 km wide, with the scale ranking second only to those formed in platform margin, is possible only when waves and ocean currents having a certain energy occur. From another perspective, it demonstrates that the formation of shallow shoals, point shoals and bioherm groups with good reservoir performance within the range of the front slope of over 350 km wide requires a quite low inclination of slope.

3   Sedimentary characteristics of each facies belt

(1)   Platform evaporite facies

The poor connectivity between the platform and open sea, coupled with the hot and dry climate, all add up to the intense evaporation in this facies belt. The anhydrite gypsum microcrystalline dolomite and marl are widely developed (Figures 4 and 9). It is similar to the sedimentary environment of sabkha and salina in the "Tucker (1985) [8]" model and the evaporate platform in the arid climate in the "Wilson (1975) [5]" model.

(2)   Restricted platform

It is a relatively closed shallow water body with lower hydrodynamic energy and a water depth of less than one meter to tens of meters. The lithology is dominated by the interbedding assemblages of thin-layered gray-dark gray micrite and granular wackestone (Figures 4 and 9). It is similar to the restricted platform in the "Wilson (1975) [5]" model, post-shoal lagoon and carbonate mud

in the "Tucker (1985) [8]" model, and the tidal flat and lagoon in the isoclinal slope in the "Read (1985) [9]" model.

(3)　Open platform

　　The water depth in this facies belt is several meters to tens of meters, the water here is actively circulated and the salinity is normal. It contains rich biological types, including gastropods, lamellibranchia, echinoderms, foraminifers and a variety of algae. It is mainly composed of subtidal low-energy environment and high-energy shoal environment (Figures 4 and 9). Among them, the subtidal low-energy environment is similar to the lagoon in open sea platform in the "Wilson (1975) [5]" model, and the sedimentary environment of euxinic lime in the "Tucker (1985) [8]" model. It mainly contains micrite and bioclastic wackestone; the high-energy shoal environment is similar to the shallow carbonate sand shoal in the "Tucker (1985) [8]" model. In addition, it is similar to the combined shallow environment of shoals or ooids (aggregates) in the isoclinal slope in the "Read (1985) [9]" model. The lithologies consist of intraclastic grainstone, ooidal grainstone and bioclastic grainstone.

(4)　Platform margin facies

　　The sedimentary characteristics in this facies belt is similar to the platform margin shoal+ platform margin reefs in the "Wilson (1975) [5]" model, to the carbonate shoals and/or continent shelf reefs in the "Tucker (1985) [8]" model, to the sedimentary-type continent shelf margin facies belt in the "Mcllreath and James (1979) [6]", to the continent margin in the "Basilone (2016) [16]"model.

　　The high-energy position in this facies belt is different from that in the nearshore continental slope break (the so-called first slope break of onshore) in the isoclinal slope in the "Read (1985) [9]" model. It is located in the slope break of rimmed platform distant to the continent (the so-called second slope break of the shelf margin). It is the strongest hydrodynamic sedimentary environment with a depth of several meters to tens of meters. There is a strong reworking under this hydrodynamic condition and it is the transformation zone of deepwater and shallow water sedimentations. There are the developments of two facies types, the platform margin reefs and platform margin shoal.

(1)　Platform margin shoal: jointly controlled by wave and tidal action, it shows extremely strong hydrodynamic conditions, good circulation of seawater, adequate oxygen and normal salinity. However, it is not suitable for the dwelling and propagation of marine benthonic organisms because the substrate is in a mobile state. Therefore, it is not adaptable to marine benthonic organisms. Mainly, there are the developments of bioclastic grainstone, intraclastic grainstone and ooidal grainstone. In addition, it develops a small amount of wackestone and micrite in intra-shoal low-energy belt.

(2)　Platform margin reefs: it is distributed along the platform margin in groups. Vertically, the reefs often co-exist with the biological debris shoals, forming reefs and shoal complexes or using the platform margin shoal as the growth base. This is different from development relationship in platform reef and in shoal front in the "Wilson (1975) [5]" model. The lithology is mainly composed of thick rudist bivalve framestone and boundstone, with a small amount of coral boundstone and coral-rudist bivalve framestone. In addition, the biological framework components include thick-shelled clams, coral, moss, algae and the likes, and there are filled by micritic calcite.

(5)　Gentle ramp facies belt in platform front

　　The location is equivalent to the platform front ramp + deep shelf margin + shelf in the "Wilson (1975) [5]" model, front ramp in the "Mcllreath and James (1979) [6]" model and "Tucker (1985) [8]" model, relatively deep ramp facies belt in isoclinal slope in "Read (1985) [9]".

　　In the study area, this facies belt is evidently characterized by the development of extremely wide and gentle slope in deep continent shelf. The slope break zone is not obvious. However, based on

the large-scale sedimentary assemblage of reefs and shoals, the gravitational flow is not developed. The depositional environment extends from near wave base of rimmed platform margin to the deeper waters or the one below maximum storm wave base. It is different from the sedimentary models proposed by previous scholars; the platform front slope belt is an obvious narrow facies belt with common development of calcareous gravity flow deposition controlled by steep terrain in the "Wilson (1975) [5]", "Mcllreath and James (1979) [6]", "Tucker (1985) [8]", and "Basilone (2016) [16]" models. There is no development of slope break and only the existence of lagoon-tidal flat facies sedimentary facies equivalent to restricted platform after the assemblage of reef and shoal facies in the isoclinal slope in the "Read (1985) [9]" model. In addition, the "front slope" in the "gentle slope-rimmed carbonate platform" model includes two depositional environments, the upper slope and the lower slope. The upper slope is located near the wave base or slightly deeper. There are the developments of shoal and point reefs, which are representatives of highlands in the slope, even large-scale independent platform (or atoll). The water depth of the lower slope is up to several hundred meters, and it is mainly composed of micrite, with a small amount of wackestone and mudstone.

(6)　Basin facies

There are two types of sedimentary facies in the basin. One is an early deepwater basin with deep water and low energy. It is similar to the sedimentary features of basin mentioned in the "Wilson (1975) [5]", "Tucker (1985) [8]", and "Read (1985) [9]" models. The lithology is mainly composed of dark micrite and mudstone, which is rich in organic matter and mud lamina. The second is the occluded gulf basin in late period, and this type is different to abyssal basin. Its genesis is related to the occluded gulf basin with lagoonal character directly transformed from the strongly occluded seawater in the basin resulted from large-scale sea level decline at the end of the Oxford stage. The water body energy is extremely low, and the biological fossils are rare. It is a thin high gamma mudstone with a thickness of only 10–20 m, with a few thin layers of gray black micrite and mudstone.

5. Origin of "Carbonate Ramp-Rimmed Platform" Reservoir

In the "carbonate reef-rimmed platform" model, reservoirs develop broadly over the open platform, platform margin and upper front ramp facies belt. In particular, open platform and platform margin facies share similar reservoir characteristics with other carbonate sedimentary models. The major differences between them are the presence of a variety of grain banks, point reefs and bioherms formed in relatively strong hydrodynamic condition in the upper front ramp, which enables the formation of reservoirs with good physical properties. Hence, an outstanding feature of the "carbonate ramp-rimmed platform" model, which makes it different from the classic platform model, is the possibility of the formation of reservoirs in the upper front ramp in marine carbonate sedimentary province. A discussion on the genesis and major controlling factors of high-quality reservoirs in the upper front ramp is presented in the following section with a case study from the Callovian-Oxfordian in the Amu Darya Basin.

5.1. Favorable Sedimentary Microfacies for Reservoir Formation

Water body energy in the upper part of the Callovian-Oxfordian front ramp in the Amu Darya Basin was sufficient enough for sedimentation of porous carbonates with particular structure and reef structure, thereby laying a material basis for formation of reservoirs. Reservoir space of point reef, shallow shoal and bioherm limestones in the upper part of the front ramp predominately consists of residual primary intergranular pores, organic framework pores and intergranular enlarged dissolved pores (Figure 10a–c), and intergranular and intragranular dissolved pores present locally (Figure 10a–c), molded pores (Figure 10b) and fractures (Figure 10d). The reservoirs here have good physical property: with the porosity ranging from 1.1% to 19.0%, averaging 7.9%, (6% to 12%, accounting for 59% of total samples); with permeability from $<0.1 \times 10^{-3}$ μm^2 to 10×10^{-3} μm^2. In addition, local maximum reached up to 74.7×10^{-3} μm^2, averaging 3.0×10^{-3} μm^2. Relative index of porosity to

permeability is 0.48 (Figure 11). Capillary pressure curve exhibits a platform-shaped segment that is slightly concave to the left (Figure 12), median radius of throat is 0.22 μm, sorting coefficient is 2.13, indicating a relatively poor sorting, skewness coefficient is 0.16, implying unimodal skewness with small slanting degree, and pore-throat structure is the combination of moderate pore and small throat. The reservoir type is therefore classified as fractured to porous type with moderate porosity and moderate to low permeability.
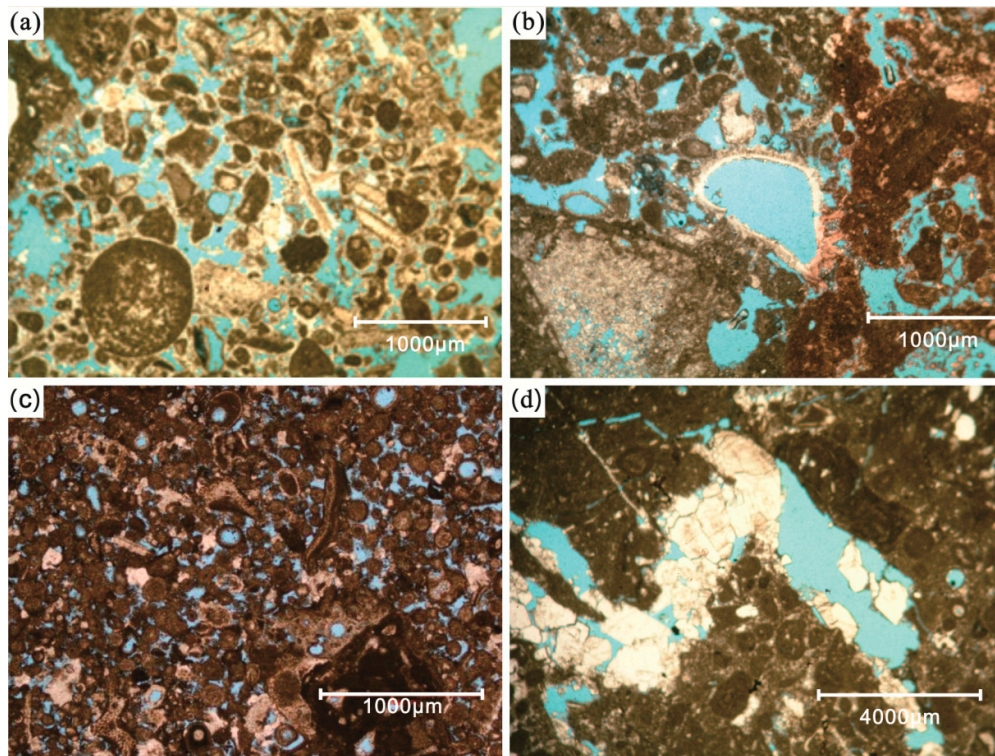
Figure 10. Types of reservoir space in the fore ramp of Callovian-Oxfordian Stage. (**a**) Intraclastic bioclastic grainstone, with residual primary intergranular pores, intergranular dissolved pores, intragranular dissolved pores and mold pores, XVa1, 3158.61 m, Well Pir-21, front ramp bioclastic shoal, casting thin section (-); (**b**) Intraclastic bioclastic grainstone, with intergranular dissolved pores, intragranular dissolved pores and molded pores, XVa1, 3158.6 m, Well Pir-21, front ramp bioclastic shoal, casting thin section (-); (**c**) Ooidal grainstone, with residual primary intergranular pores, intergranular dissolved pores, intragranular pores and mold pores, XVm, 3791.0 m, Well Oja-21, front ramp ooidal shoal, casting thin section (-); (**d**) Lump packstone, with framework dissolved pores and dissolved fractures, XVa1, 3552.17 m, Well Cha-21, front ramp mound, casting thin section (-).
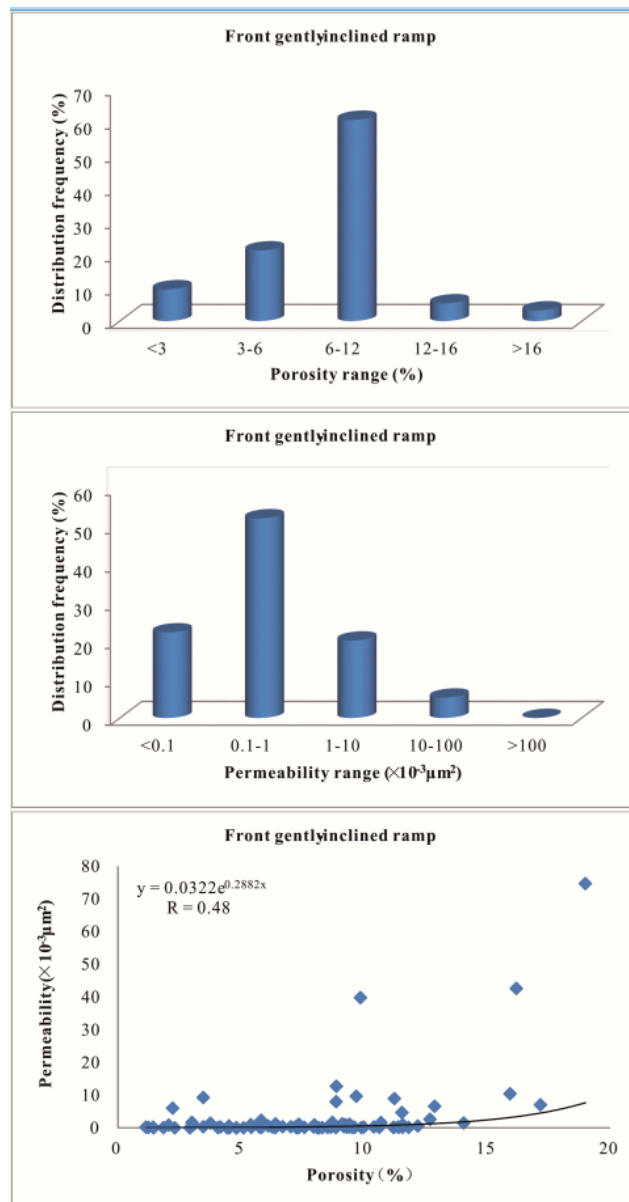
Figure 11. Physical properties of reservoirs and correlation plot between porosity permeability of Callovian-Oxfordian Stage.
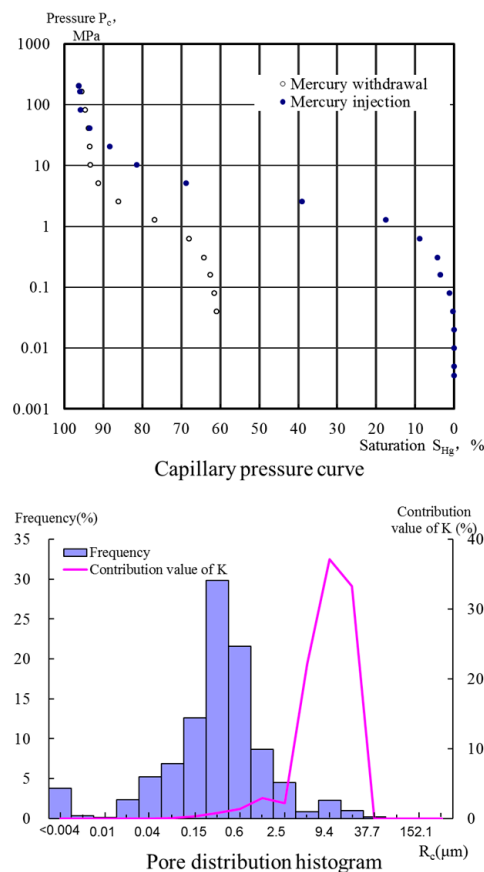
Figure 12. Plot showing capillary pressure curve of Callovian-Oxfordian Stage.

5.2. Dissolution Role is Reservoir Formation

In addition to abundant residual primary intergranular porosity, reef and shoal reservoirs facies in the upper part of the Callovian-Oxfordian front ramp in the Amu Darya Basin contain numerous dissolution-formed secondary pores resulted from dissolution. According to the analysis of thin sections, electron probe, and X-ray diffraction data of interstitial substance, the morphology and filling sequence of minerals can indicate the sequence of dissolution. In addition, the dissolution can be divided into three stages.

5.2.1. Early Diagenesis Dissolution

Early diagenesis dissolution occurred mainly in the near-surface environment and, due to the effect of fresh water, the reservoir space of composite reef-shoal was dominated by intragranular porosity, i.e., dissolved and mold pores formed by selective dissolution. Pores formed by this dissolution are mostly filled at later-stage diagenesis and hence contributed very little to effective reservoir space. However, some residual pores could provide dissolution pathway for late dissolution and hence could accelerate the occurrence of dissolution, thereby laying the basis for the formation of good-quality reservoir space during the later-stage dissolution and superimposed reformation of preexisting pores. The reservoir volumes space formed at this stage consists of predominately residual primary intergranular pores and organic framework pores.

5.2.2. Middle Diagenesis Early-Stage Dissolution

Middle diagenesis dissolution occurred in a relatively closed to semi-closed system. Intensive diagenetic fracturing, dissolution and burial dolomitization began to occur in localized areas at this period, which enabled the formation of new pore, vug and fracture system. The effects of diagenetic

fracturing and burial dolomitization were limited, and the dissolution was predominately non-selective type, forming numerous irregular late pores. Although rendering formation and enlargement of some reservoir space, this dissolution also reduced some reservoir space by filling pores with secondary minerals including calcite (0.3–2 mm) (Figure 13a–c), dolomite (Figure 13d–e), anhydrite (Figure 13f), fluorite (Figure 13g) and celestite (Figure 13h). During this period, reservoir space type was dominated by residual primary intergranular pores and organic framework pores, and reservoir property was improved significantly as a result of superimposition of a large variety of secondary pores.
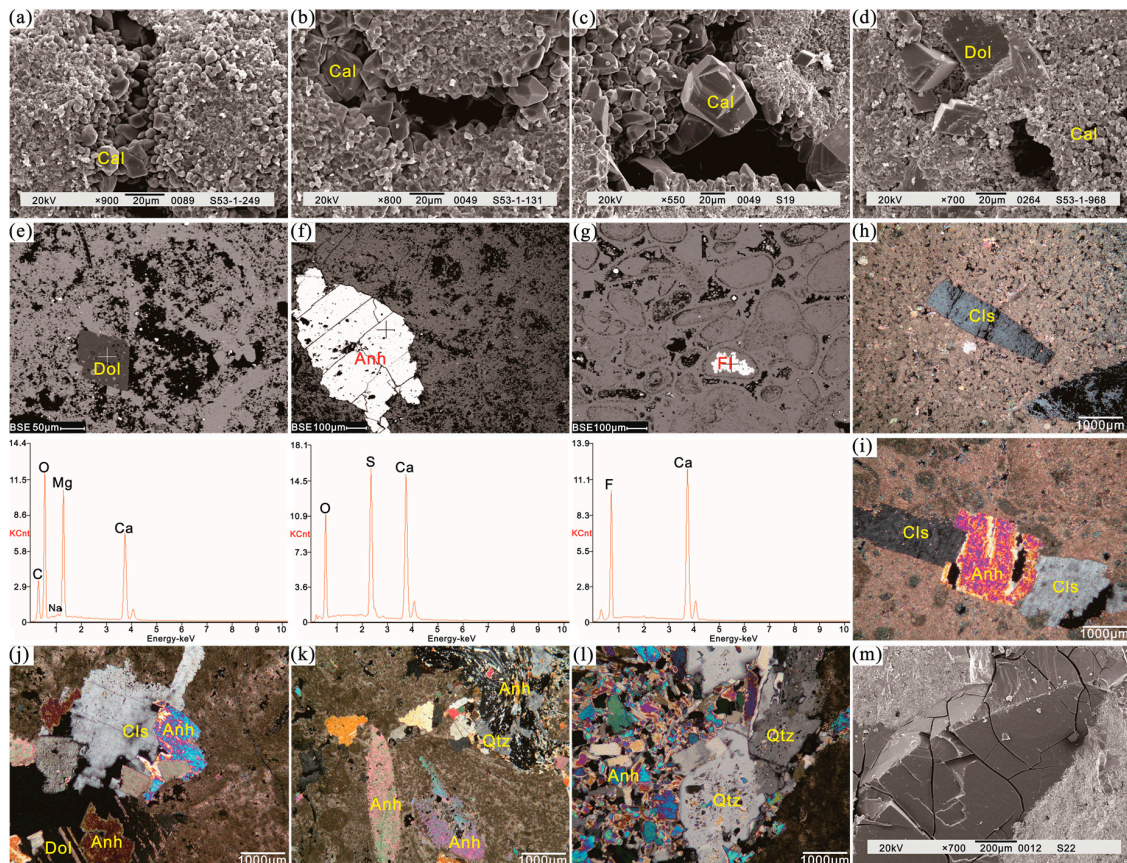
Figure 13. Typical microscopic photographs of mineral types and their syngenetic sequence. (**a**) Intergranular pores filled with calcite crystals, peloid packstone, 2404.23 m, XVp, SEM; (**b**) Intergranular pores partially filled with secondary calcite crystals, bioclastic packstone, 2384.35 m, XVp, SEM; (**c**) Primary skeletal pores partially filled with secondary calcite crystals, and the horse—tooth—shaped secondary calcite crystals grew along the pore walls, bioclastic wackestone, 2491.79 m, XVm, SEM; (**d**) Secondary rhombic dolomite shows intact crystal shape, micrite, 2519.92 m, XVhp, SEM; (**e**) Dolomite, Surrounding rocks are bioclastic wackestone, 2492.37 m, XVhp, EPMA; (**f**) Anhydrite, Surrounding rocks are bioclastic grainstone, 2410.08 m, XVp, EPMA; (**g**) Fluorite, Surrounding rocks are bioclastic packstone, 2445.35 m, XVm, EPMA; (**h**) Celestite, peloid packstone, 2399.3 m, XVp, casting thin section (+); (**i**) The syngenetic sequence of minerals is the follows: anhydrite → celestite, peloid packstone, 2399.3 m, XVp, casting thin section (+); (**j**) The syngenetic sequence of minerals is the follows: dolomite → anhydrite → celestite, bioclastic wackestone, 2518.05 m, XVhp, casting thin section (+); (**k**) The syngenetic sequence of minerals is the follows: anhydrite → quartz, bioclastic wackestone, 2518.27 m, XVp, casting thin section (+); (**l**) The syngenetic sequence of minerals is the follows: anhydrite → quartz, bioclastic wackestone, 2518.27 m, XVp, casting thin section (+); (**m**) Fractures filled with bitumen, bioclastic wackestone, 2492.685 m, XVm, SEM.

5.2.3. Middle Diagenesis Late-Stage Dissolution

The strata have been consolidated in this period, and thus, consolidation, pressure dissolution and cementation were weakened greatly and had little influence on the reservoir. However, reformation of reservoirs resulted from dissolution and tectonic disruption was strengthened, which, together with the tectonic disruption and dissolution, diagenetic alteration (e.g., the formation of anhydrite, celestite and silicification (Figure 13i–l), precipitation and filling of secondary minerals, and the continually strengthening of filling of late-stage bitumen (Figure 13m), caused reduction of partial reservoir space. In general, however, physical properties of reservoirs became better at this period, since new structural fractures were formed and preexisting pores, vugs and fractures continued to be dissolved and enlarged, providing effective space for hydrocarbon migration and accumulation. As a result, good to excellent reservoir properties could be formed in a certain scope.

5.3. Case Study of Reef and Shoal in the Upper Ramp

Well Oja-21 is in the central-southern part of the study area (Figure 3), in which SQ2 sequence includes shoal, mound and slope mud of the upper ramp subfacies. The shoal includes the bioclastic shoal, oolitic shoal and intraclastic shoal. Grainstone depositing in relatively high-energy environment contains abundant reservoir space: i.e., primary intergranular pores, intergranular enlarged dissolved pores, intragranular dissolved pores, molded pores and fractures (Figure 10c). Intraclastic shoal has the best reservoir properties: with a porosity range from 5.9% to 16.2%, averaging 10.2%, and the permeability range from 0.37 to 42.6×10^{-3} μm^2, averaging 22.69×10^{-3} μm^2. Bioclastic shoal and oolitic shoal have fairly good physical properties and the reservoirs formed are predominately porous-type (Table 1). Physical property of mound is worse than those shoals: with the porosity ranging from 4.8% to 12.2%, averaging 9.5%, and the permeability ranging from <0.01 to 1.59×10^{-3} μm^2, averaging 0.44×10^{-3} μm^2, and the reservoirs formed are predominately porous- and fractured-type. Inter-shoal and slope mud deposited in low-energy environment commonly have poor physical properties, and the reservoir in this facies with hydrocarbon shows is fractured-type reservoir with few pores.

Table 1. Values of porosity and permeability from different environment of the front gently inclined ramp in Well Oja-21.

Facies Belt		Front Gently-Inclined Ramp					
Microfacies		**Oolitic Shoal**	**Intraclastic Shoal**	**Bioclastic Shoal**	**Mound**	**Intershoal**	**Slope Mud**
		(*n* = 8)	(*n* = 19)	(*n* = 14)	(*n* = 28)	(*n* = 9)	(*n* = 13)
Porosity (%)	Range	5.8–14.1	5.9–16.2	6.4–19.0	4.8–12.2	2.9–10.7	1.5–11.6
	Mean	9.4	10.2	12.2	9.5	6.3	5.9
Permeability ($\times 10^{-3}$ μm^2)	Range	0.07–12.7	0.37–42.6	0.15–74.7	<0.01–1.59	<0.01–0.55	<0.01–0.55
	Mean	4.28	22.69	12.04	0.44	0.16	0.08

6. Conclusions

(1) Based on petrological, paleontological and seismic studies of the Callovian and Oxfordian, in combination with regional geological characteristics and sedimentary setting, an appropriate sedimentary model of "carbonate ramp-rimmed platform" has been proposed and established, and detailed demonstration, description and comparison of concept, evidence and feature of this model with other classic models are presented.

(2) In addition to intra-platform shoals and point reefs in open platform, and reefs and shoals in platform margin, according to the sedimentary model of "carbonate ramp-rimmed platform", the upper slope shoals, point reefs and mound groups in front ramp allow for the formation of reservoirs with good physical properties too. The reservoir space is dominated by primary intergranular pores, organic framework pores and intergranular enlarged dissolved pores, and the reservoirs are fractured and porous type.

(3)　Sedimentary microfacies and diagenesis are the main factors controlling the formation of high-quality reservoirs. Upper slope shoals, point reefs and mound of front ramp are deemed to be the material basis for the formation of high-quality reservoirs, while dissolution and fracture mainly occurred at different periods are critical to the formation of high-quality reservoirs.

Author Contributions: Wenli Xu and Huaguo Wen conceived and designed; Wenli Xu, Rongcai Zheng, Fei Huo, Mingcai Hou and Gang Zhou analyzed the data; Wenli Xu, Huaguo Wen and Fengjie Li contributed materials; Wenli Xu wrote the paper and led research.

Conflicts of Interest: The authors declare no conflict of interest.

References

1.　Gu, J.Y.; Ma, F.; Ji, L.D. Types, characteristics and main controlling factors of carbonate platform. *J. Palaeogeogr.* **2007**, *11*, 21–27.

2.　Shaw, A.B. *Time in Stratigraphy*; McGraw-Hill: New York, NY, USA, 1964; p. 365.

3.　Irwin, M.L. General theory of epeiric clear water sedimentation. *Bull. AAPG* **1965**, *49*, 445–459.

4.　Laporte, L.F. Recognition of a transgressive carbonate sequence within an epeiric sea: Helderberg Group (Lower Devonian) of New York State. *AAPG Bull.* **1967**, *14*, 98–119. [CrossRef]

5.　Wilson, J.L. *Carbonate Facies in Geologic History*; Springer: New York, NY, USA, 1975; pp. 229–233.

6.　Mcllreath, I.A.; James, N.P. Facies models Carbonate slopes. *Geosci. Can.* **1979**, *5*, 184–199.

7.　Tucker, M.E. *Sedimentary Petrology: An Introduction*; Blackwell Scientific Publications: Oxford, UK, 1981; pp. 19–27.

8.　Tucker, M.E. *Shallow-Marine Carbonate Facies and Facies Models*; Blackwell Scientific Publications: Oxford, UK, 1985; pp. 147–169.

9.　Guan, S.C. *The Change of Sea and Land, Sedimentary Facies in Sea Area and Oil & Gas in China*; Science Press: Beijing, China, 1984; pp. 1–104.

10.　Read, J.F. Carbonate platform facies models. *AAPG Bull.* **1985**, *69*, 1–21.

11.　Santantonio, M. Facies associations and evolution of pelagic carbonate platform/basin systems: Examples from the Italian Jurassic. *Sedimentology* **1993**, *40*, 139–1067. [CrossRef]

12.　Bosence, D.; Cross, N.; Hardy, S. Architecture and depositional sequences of Tertiary fault-block carbonate platforms; an analysis from outcrop (Miocene, Gulf of Suez) and computer modeling. *Mar. Pet. Geol.* **1998**, *15*, 203–221. [CrossRef]

13.　Bosence, D. A genetic classification of carbonate platforms based on their basinal and tectonic settings in the Cenozoic. *Sediment. Geol.* **2005**, *175*, 49–72. [CrossRef]

14.　Basilone, L. Mesozoic tectono-sedimentary evolution of Rocca Busambra in western Sicily. *Facies* **2009**, *55*, 115–135. [CrossRef]

15.　Basilone, L.; Morticelli, G.M.; Lena, G. Mesozoic tectonics and volcanism from Tethyan rifted continental margins in western Sicily. *Sediment. Geol.* **2010**, *226*, 54–70. [CrossRef]

16.　Basilone, L.; Sulli, A. A facies distribution model controlled by a tectonically inherited sea bottom topography in the carbonate rimmed shelf of the Upper Tithonian-Valanginian Southern Tethyan continental margin (NW Sicily, Italy). *Sediment. Geol.* **2016**, *342*, 91–105. [CrossRef]

17.　Basilone, L.; Sulli, A.; Gasparo Morticelli, M. Integrating facies and structural analyses with subsidence history in a Jurassic-Cretaceous intraplatform basin: Outcome for paleogeography of the Panormide Southern Tethyan margin (NW Sicily, Italy). *Sediment. Geol.* **2016**, *339*, 258–272. [CrossRef]

18.　Basilone, L.; Perri, F.; Sulli, A.; Critelli, S. Paleoclimate and extensional tectonics of short-lived lacustrine environments. Lower Cretaceous of the Panormide Southern Tethyan carbonate platform (NW Sicily). *Mar. Pet. Geol.* **2017**, *88*, 428–439. [CrossRef]

19. Chen, J.S.; Wang, Z.Y.; Dai, Z.Y. Study of the Middle and Upper Ordovician rimmed barbonate platform system in the Tazhong area, Tarim basin. *J. Palaeogeogr.* **1999**, *1*, 8–17.
20. Chen, M.; Xu, X.S.; Wan, F. Study on outcrop sequence stratigraphy of the Lower-Middle Ordovician strata in Keping, Tarim basin. *Acta Sedimentol. Sin.* **2004**, *22*, 110–116.
21. Guo, Y.Q.; Liu, L.F.; Zhu, S.L. Classification and assessment of petroleum system in Amu-Daria Basin. *Pet. Explor. Dev.* **2006**, *33*, 515–520.
22. An, Z.X.; Hu, Z.Q. *Oil and Gas Area of Mid-Aisa*; Petroleum Industry Press: Beijing, China, 1993; pp. 41–216.
23. Che, Z.C.; Luo, J.H.; Liu, L. The Basic Structure Classification and Genetic Analyses of Oil and Gas-bearing Basins in Central Asia and Northwestern China. *Acta Geosci. Sin.* **1997**, *18*, 113–121.
24. Jia, C.Z.; Yang, S.F.; Chen, H.L. *Structural Geology and Natural Gas in the Northern Magin Basin Group*; Petroleum Industry Press: Beijing, China, 2001; pp. 136–143.
25. Qiu, D.Z.; Xie, Y.; Li, X.Q. Geological Characteristics of Lithofacies Paleogeography and Hydrocarbon Accumulation in Asian Tethyan Tectonic Domain. *Mar. Pet. Geol.* **2009**, *14*, 41–50.
26. Xu, W.S.; Liu, X.L.; Yu, Z.Q. Geological Structure of Amu-Darya Basin in Central Asia. *Nat. Gas Geosci.* **2009**, *20*, 744–748.
27. Zhang, X.Y. *Optimization of Exploration Targets and Study on Hydrocarbon Accumulation Rules for CNPC Cooperative Blocks of the Amu Darya Basin*; Petroleum Exploration and Development Research Institute: Beijing, China, 2012.
28. Nie, M.L.; Wu, L.; Xu, S.B. Genetic mechanism and exploration significance of tectonic action in the Bieshikent Depression and its adjacent area in the Amu-Darya Basin. *Nat. Gas Ind.* **2013**, *33*, 45–50.
29. Ulmishek, G.F. *Petroleum Geology and Resources of the Amu-Darya Basin, Turkmenistan, Uzbekistan, Afghanistan and Iran*; U.S. Geological Survey Bulletin 2201–H, 2004; pp. 1–38.
30. Zhang, Z.W.; He, Y.Y.; Wang, C.S. Structural Characteristics and Evolution of Chardzhou and Bukhara Terraces in Amu-Darya Basin, Middle Asia. *Mar. Pet. Geol.* **2010**, *15*, 48–56.
31. Meisel, T.; Krahenbuhl, U.; Michael, A.N. Combined osmium and strontium isotopic study of the Cretaceous-Tertiary boundary at Sumbar, Turkmenistan: Atest for an impact vs. a volcanic hypothesis. *Geology* **1995**, *5*, 313–316. [CrossRef]
32. Qi, B.Q.; Ran, Z.B.; Wang, X.Q. Identification of limestone reservoirs and prediction of their fluid properties in the Amu Darya Right Bank Block, Turkmenistan. *Nat. Gas Ind.* **2011**, *30*, 21–25.
33. Zhang, B.; Zheng, R.C.; Liu, H.N. Characteristics of Carbonate Reservoir in Callovian-Oxfordian of Samandepe Gasfield, Turkmenistan. *Acta Geol. Sin.* **2010**, *84*, 117–125. [CrossRef]
34. Dong, X.; Zheng, R.C.; Wu, L. Diagenesis and porosity evolution of carbonate reservoirs in Samandepe Gas Field, Turkmenistan. *Lithol. Reserv.* **2010**, *22*, 54–61.
35. Li, H.W.; Tong, X.G.; Wang, S.H. An analysis of geological characteristics and exploration potential of the Jurassic play, Amu Darya Basin. *Nat. Gas Ind.* **2011**, *30*, 6–12.
36. Zheng, R.C.; Zhao, C.; Liu, H.N. Cathodoluminescence and its significance of the Callovian-Oxfordian carbonate rocks in Amu Darya basin, Turkmenistan. *J. Chengdu Univ. Technol. (Sci. Technol. Ed.)* **2010**, *37*, 377–385.
37. Xu, W.L.; Zheng, R.C.; Fei, H.Y. The sedimentary facies of Callovian-Oxfordian Stage in Amu Darya basin, Turkmenistan. *Geol. China* **2012**, *39*, 954–964.
38. Wang, Q.; Yan, X.; Xu, W.L. Sequence-Paleogeographic Characteristics and Evolution of Callovian- Oxfordian in Amu Darya Basin, Turkmenistan. *Geol. Explor.* **2014**, *50*, 795–804.
39. Dickson, J.A.D. Carbonate identification and genesis as revealed by staining. *J. Sediment. Petrol.* **1966**, *36*, 441–505.
40. Dunham, R.H. *Classification of Carbonate Rocks, According to Depositional Texture*; Ham, W.E., Ed.; Classification of Carbonate Rocks; AAPG Memoir: Tulsa, OK, USA, 1962; pp. 108–121.
41. Carozzi, A.V. *Sedimentary Petrology*; Prentice Hall: Englewood Cliffs, NJ, USA, 1993; p. 263.
42. Tucker, M.E.; Wright, V.P. *Carbonate Sedimentology*; Blackwell: Oxford, UK, 1990; p. 482.
43. Flügel, E. *Microfacies of Carbonate Rocks: Analysis, Interpretation and Application*, 2nd ed.; Springer: Berlin, Germany, 2010; p. 984.
44. Vail, P.R.; Mitchum, R.M., Jr.; Thompson, S., III. *Seismic Stratigraphy and Global Changes of Sea Level, Part 4: Global Cycles of Relative Changes of Sea Level*; Payton, C.E., Ed.; Seismic Stratigraphy-Applications to Hydrocarbon Exploration; AAPG Memoir: Tulsa, OK, USA, 1977; pp. 83–98.

45. Vail, P.R.; Mitchum, R.M., Jr. *Seismic Stratigraphy and Global Changes of Sea Level, Part 3: Relative Changes of Sea Level from Coastal Onlap*; Clayton, C.E., Ed.; Seismic Stratigraphy-Applications to Hydrocarbon Exploration; AAPG Memoir: Tulsa, OK, USA, 1977; pp. 63–81.

46. Haq, B.U.; Hardenbol, J.; Vail, P.R. *Mesozoic and Cenozoic Chronostratigraphy and Cycles of Sea-Level Change*; Wilgus, C.K., Hastings, B.S., Kendall, C.G., Posamentier, H.W., Ross, C.A., Van Wagoner, J.C., Eds.; Sea-Level Changes—An Integrated Approach; SEPM Special Publications: Tulsa, OK, USA, 1988; Volume 42, pp. 71–108.

47. Zheng, R.C.; Liu, H.N.; Wu, L. Geochemical characteristics and diagenetic fluid of the Callovian-Oxfordian carbonate reservoirs in Amu Darya basin. *Acta Petrol. Sin.* **2012**, *28*, 961–970.

48. Wen, H.G.; Gong, B.S.; Zheng, R.C. Deposition and diagentic system of carbonate in Callovian-Oxfordian of Samandepe Gasfield, Turkmenistan. *J. Jilin Univ. (Earth Sci. Ed.)* **2010**, *42*, 991–1002.

49. Xu, W.L. Sedimentary mode of glacis carbonate platform-taking Callovian-Oxfordian of Upper-Middle Jurassic in Amu-Darya basin of Turkmenistan as an example. Ph.D. Dissertation, Chengdu University of Technology, Chengdu, China, 2013; pp. 20–46.

50. Cao, J.; Xu, M.; He, Z.H. An analysis of pore fluid sensitivity parameters in reef limestone reservoirs: An example from Callovian-Oxfordian carbonate reef reservoirs in the Amu Darya Right Bank Block, Turkmenistan. *Nat. Gas Ind.* **2010**, *30*, 37–40.

51. Lu, B.X.; Zheng, R.C.; Chen, S.C. Characteristics of carbonate reservoir in Oxfordian of Odjarly Gasfield, Amu Darya Basin. *J. Guilin Univ. Technol.* **2011**, *31*, 504–510.

52. Liu, S.L.; Zheng, R.C.; Yan, W.Q. Characteristics of Oxfordian carbonate reservoir in Agayry area, Amu Darya Basin. *Lithol. Reserv.* **2012**, *24*, 57–63.

53. Zheng, R.C.; Chen, H.R.; Wang, Q. The reservoir characteristics and their controlling factors of Callovian-Oxfordian carbonates in Amu Darya Basin. *Acta Petrol. Sin.* **2014**, *30*, 779–788.

54. Xu, W.L.; Zheng, R.C.; Fei, H.Y. Characteristics and timing of fractures in the Callovian-Oxfordian boundary of the right bank of the Amu Darya River, Turkmenistan. *Nat. Gas Ind.* **2012**, *32*, 33–38.

55. Zonenshayn, L.P.; Kuzmin, M.I.; Natapov, L.M. *Tectonics of Lithospheric Plates of the USSR (Tektonika Litosfernykh Plit Territorii SSSR), Volumes I and II*; Nedra: Moscow, Russia, 1990; pp. 328–336.

56. Sheikholeslami, M.; Kouhpeym, M. Structurale analysis and tectonic evolution of the eastern Binalud Mountains, NE Iran. *J. Geodyn.* **2012**, *61*, 23–46. [CrossRef]

57. Sengor, A.M.C. *A New Model for the Late PalaeozoiceMesozoic Tectonic Evolution of Iran and Implications for Oman*; Geological Society of London, Special Publications: London, UK, 1990; Volume 49, pp. 797–831.

58. Muttoni, G.; Mattei, M.; Balini, M.; Zanchi, A.; Gaetani, A.; Berra, F. The drift history of Iran from the Ordovician to the Triassic. In *South Caspian to Central Iran Basins*; Geological Society of London, Special Publication: London, UK, 2009; Volume 312, pp. 7–29.

59. Maksimov, S.P. *Sedimentary Cover of Central Asia and South Kazakhstan (Osadochnyi Chekhol Sredney Azii i Yuzhnogo Kazakhstana)*; Nedra: Moscow, Russia, 1992; p. 148.

60. Lyberis, N.; Manby, G. Oblique to orthogonal convergence across the Turan Block in the post-Miocene. *AAPG Bull.* **1999**, *83*, 1135–1160.

61. Thomas, J.; Cobbold, P.; Shein, V.; Douaran, S.L. Sedimentary record of Late Palaeozoic to recent tectonism in Central Asiaeanalysis of subsurface data from the Turan and South Kazakh domains. *Tectonophysics* **1999**, *313*, 243–263. [CrossRef]

62. Brookfield, M.E.; Hashmat, A. The geology and petroleum potential of the North Afghan platform and adjacent areas (northern Afghanistan, with parts of southern Turkmenistan, Uzbekistan, and Tajikistan). *Earth Sci. Rev.* **2001**, *55*, 41–71. [CrossRef]

63. Khain, V.E.; Sokolov, B.A.; Kleshchev, K.A.; Shein, V.S. Tectonic and geodynamic setting of oil and gas basins of the Soviet Union. *Am. Assoc. Petrol. Geol. Bull.* **1991**, *75*, 313–325.

64. Kavoosi, M.; Lasemi, Y.; Sherkati, S.; Moussavi-Harami, R. Facies analysis and depositional sequences of the Upper Jurassic Mozduran Formation, a reservoir in the Kopet Dagh Basin, NE iran. *J. Pet. Geol.* **2009**, *32*, 235–260. [CrossRef]

65. Taheri, J.; Fürsich, F.; Wilmsen, M. Stratigraphy, depositional environments and geodynamic significance of the Upper Bajocian Bathonian Kashafrud Formation, NE Iran. In *South Caspian to Central Iran Basins*; Geological Society of London, Special Publication: London, UK, 2009; pp. 205–218.

66. Ball, M.M. Carbonate sand bodies of Florida and the Bahamas. *J. Sediment. Petrol.* **1967**, *37*, 556–591.

67. Hine, A.C.; Wilber, R.J.; Bane, J.M.; Neumann, A.C.; Lorenson, K.R. Offbank transport of carbonate sands along open, leewardmargins; Northern Bahamas. *Mar. Geol.* **1981**, *42*, 327–348. [CrossRef]
68. Harris, P.M.; Purkis, S.; Ellis, J.; Swart, P.K.; Reijmer, J.J.G. Mapping bathymetry and depositional facies on great Bahama Bank. *Sedimentology* **2015**, *62*, 566–589. [CrossRef]